

Received: 14.08.2024

Accepted: 16.01.2025

Research Article

*Computational investigation using DFT approach and molecular docking analysis of 2-(4-methoxyphenyl)benzo[d]thiazole*

Mridula Guin<sup>a</sup>, Kodipura P. Sukrutha<sup>b</sup>, Kamakshi Sharma<sup>a</sup>, Paratpar Sarkar<sup>a</sup>, Ravani A. Roopa<sup>c,1</sup>, Maralinganadoddi P. Sadashiva<sup>d,2</sup>, Kuppalli R. Kiran<sup>d</sup>

<sup>a</sup>Department of Chemistry and Biochemistry, Sharda University, Greater Noida, Uttar Pradesh, India

<sup>b</sup>Department of Studies in Chemistry, Bharathi College Post Graduate and Research Centre (Autonomous), Bharathinagara, Mandya, Karnataka, India.

<sup>c</sup>Department of Studies in Chemistry, Pooja Bhagavat Memorial Mahajana Education Centre, University of Mysore, Mysuru, Karnataka, India

<sup>d</sup>Department of Studies in Chemistry, University of Mysore, Mysuru, Karnataka, India

**Abstract:** The electronic structure of the 2-(4-methoxyphenyl)benzo[d]thiazole was simulated using DFT calculations at B3LYP/6-311++G\*\* level. Theoretically calculated structural parameters are in good match with the experimentally reported parameters. Molecular reactivity and stability of the complex has been assessed through frontier molecular orbital analysis and also through evaluation of molecular electrostatic potential (MEP). The presence of high electron density or negative charge around the nitrogen and oxygen atom of the molecules signify the strong nucleophilic reactivity in the molecule. Further, the intermolecular contacts of the complex are analysed through Hirshfeld surface analysis and finger print plots. The nature of shape index and curvedness surface confirms the molecular crystal to be stabilized through weak  $\pi$ - $\pi$  stacking interactions. The fingerprint plots indicate  $H\cdots H$  and  $C\cdots H$  interactions as major contacts contributing about 46.7% and 29.4% respectively to the overall crystal packing. Further, the drug likeness and absorption-distribution-metabolism-excretion-toxicity (ADMET) properties of the compound is analysed to determine its potential bioactivity. ADMET studies confirms nontoxic behaviour of the compound. Molecular docking studies confirms that the molecule is stable enough to bind strongly with the two cancers receptor Metastasis factor (S100A4) and adhesion (GPCR ADGRL3) and can modulate the signalling of the cancer protein that can alter the behaviour and pattern of cancer initiation in the body.

**Keywords:** DFT, MEP, Benzothiazole, Hirshfeld surface, Cancer protein, Molecular docking.

## 1. Introduction

Benzothiazoles constitute a significant and widely occurring group of fused heterocyclic compounds [1,2]. These compounds are characterized by a benzene ring fused to a thiazole ring, which contains both sulfur and a nitrogen atom in the five-membered ring. The benzothiazole motif is prevalent in various pharmacological agents, natural products, and synthetic intermediates [3,4].

Specifically, the 2-arylbenzothiazole scaffold holds significant importance in various bioactive compounds, including antiparasitic, antituberculous, antitumor agents, antidiabetic, cardiovascular, and calcium antagonist [5]. Furthermore, 2-arylbenzothiazoles have garnered substantial interest due to their potential uses in organic luminescent materials, industrial dyes, and agrochemical compounds [6]. As a result, there has been a continuous dedication to the development of

<sup>1</sup>Corresponding Authors

e-mail: roopa13th@gmail.com

<sup>2</sup>Corresponding Authors

e-mail: [mpsadashiva@gmail.com](mailto:mpsadashiva@gmail.com)

Mridula Guin, Kodipura P. Sukrutha, Kamakshi Sharma, Paratpar Sarkar, Ravani A. Roopa, Maralinganadoddi P. Sadashiva, Kuppalli R. Kiran

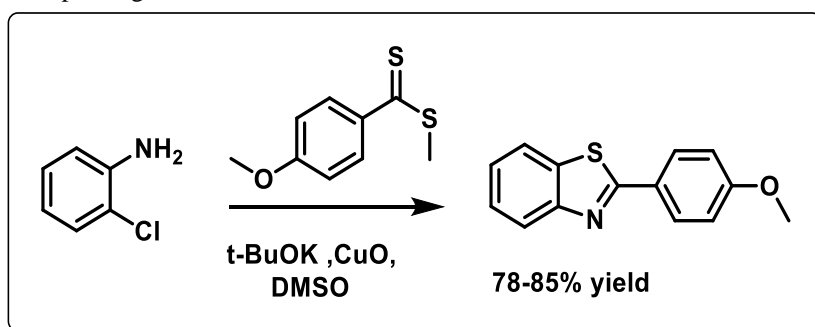
innovative synthetic methods for producing derivatives of 2-arylbenzothiazoles. As a result, the innovation of new approaches in synthesizing biologically relevant benzothiazole scaffolds is of utmost significance [7-9].

Conventional techniques for producing benzothiazoles typically involve the condensation of 2-aminothiophenols with acids, alcohols, aldehydes, and various reagents [10,11]. An alternative method includes the intramolecular annulation of thiobenzanilides using transition metals [12]. However, these conventional approaches suffer from drawbacks like multistep synthesis, limited substrate scope, and the use of expensive catalysts. To address these challenges, researchers, including Zhang [13], Wang [14], Huang [15], Zhu [16] and Jiang [17] have introduced copper-catalysed cyclization strategies for benzothiazole synthesis using 2-haloanilines. Despite advancements, these approaches still face limitations, such as prolonged reaction times, harsh

conditions. In a recent article [18], the emphasis was on synthesizing benzothiazoles using dithiocarbonates in conjunction with a palladium catalyst. Building on this foundation, our research introduces a copper-mediated synthesis of benzothiazoles utilizing dithioesters.

This endeavor extends our prior work, dedicated to developing novel methodologies for synthesizing biologically significant N-heterocycles from organosulfur dithioesters. Our study presents an efficient and innovative approach to synthesizing benzothiazoles from dithioesters. The one-component tandem cyclization enables the selective formation of 2-(4-methoxyphenyl) benzo[d]thiazole from 2-chloroaniline and methyl 4-methoxybenzodithioate using copper oxide (Scheme 1).

The reaction is not only effective and facile but is also conducted in a one-pot manner under mild conditions.



**Scheme 1.** Synthesis of 2-(4-methoxyphenyl) benzo[d]thiazole

Over the past few years computational chemistry is a fast-evolving discipline that support analyzing chemical observations in a molecular level [19,20]. We performed the computational studies of the compound to understand its chemical properties and reactivity characteristics using DFT approach. Moreover, we have carried out a molecular docking analysis of the compound with four therapeutic cancer protein targets to predict the binding pattern and energy. Cancer cells spread from one part of the body to the other through the process of metastasis. S100A4 also known as mts1 is a member of S100 family of Ca<sup>2+</sup> binding proteins that is directly involved in tumor invasion and metastasis via interactions with specific protein targets including non muscle myosin II A [21]. It is associated with nasopharyngeal carcinoma [22]. Other cancer proteins particularly GPCR is also

responsible for the formation and initiation of metastatic cancer [23]. G-protein-coupled receptors (GPCRs) are a class of integral membrane proteins that detect environmental cues and trigger cellular responses. GPCRs are known to modulate the processes such as proliferative signalling, replicative immortality, evasion of growth suppressors, resistance to apoptosis, initiation of angiogenesis, and activation of invasion and metastasis that are identified as the hallmarks of cancer [24,25].

## 2. Computational Method

### 2.1. Density Functional Theory (DFT) study

All quantum chemical calculations are carried out using Gaussian 16 program package [26]. The ground state geometry of the compound was determined using DFT calculation by B3LYP

Mridula Guin, Kodipura P. Sukrutha, Kamakshi Sharma, Paratpar Sarkar, Ravani A. Roopa, Maralinganadoddi P. Sadashiva, Kuppalli R. Kiran

functional in conjunction with 6-311++G\*\* basis set. The B3LYP functional is extensively used to obtain reliable geometry and energetic properties with limited computational cost [27, 28]. The diffused and polarized Pople basis set allow for flexibility of molecular orbitals for improved results. The convergence criteria were maintained at default level without any constraint on the geometry. Geometry optimization was followed by frequency calculation at the same level of theory to confirm the stationary point as a true energy minimum. The visualization of the electronic structure was done using Gaussview 6.0 program. Absence of imaginary frequency during vibrational calculation confirmed the optimized geometry as true minima on the potential energy surface. Energy of HOMO (Highest Occupied Molecular Orbital), LUMO (Lowest Unoccupied Molecular Orbital) and band gap is determined to understand the chemical reactivity of the compound. Moreover, molecular electrostatic potential of the compound is calculated from the electron density to predict the electrophilic and nucleophilic regions in the complex.

## 2.2. Molecular Hirshfeld surface analysis

Hirshfeld surface analysis is widely used tool for understanding the intermolecular interactions in a molecular crystal. The intermolecular close contacts can be visualized qualitatively and quantitatively through the Hirshfeld surface. The red-white-blue colour surface of the normalized contact distance  $d_{\text{norm}}$  identifies the close contacts around van der waals radius, short contacts and long contacts. The mapped  $d_{\text{norm}}$  surface shows red spots wherever close contacts are present in the molecular crystal.

Crystal Explorer 17.5 program [29] is used to perform Hirshfeld surface (HS) analysis of the complex using the cif file. Three colour coded surface e.g.  $d_{\text{norm}}$ , shape index and curvedness were mapped for the molecular crystal. The Hirshfeld surface was generated using a high standard surface resolution. All the surfaces were presented in a transparent mode for clear visualization. Additionally, 2D fingerprint plots in terms of  $d_e$  and  $d_i$  are determined to summarize the nature and type of intermolecular contacts used in packing of the molecular crystal.

## 2.3. Molecular Docking

Molecular docking software I GEMDOCK was used to carry out docking procedure [30]. To initially validate the pharmacological interactions, we selected four therapeutic protein targets, viz, Ca<sup>2+</sup>-Bound Activated Form of the S100A4 Metastasis Factor (PDB code 2q91 [21], MRCK beta in complex with fasudil (PDB code 3tku) [22], an engineered Axl 'decoy receptor (PDB code 4ra0) [23], adhesion GPCR (PDB code 8jmt) [24], because these proteins were well studied. The ligand in SDF format was taken for molecular docking analysis. Binding site of the target protein were prepared. Water molecules were removed from all the proteins. Protein- ligand complexes were generated using I GEMDOCK. After docking protein-ligand interaction profiles were generated. After that pharmacological were generated by profiles.

## 3. Results and discussion

### 3.1. Geometry

The optimized geometry of the molecule is shown in **Figure 1**. The computed structural parameters of the molecule are listed in **Table 1**. The computed bond distance and angles are in good agreement with the experimental geometrical parameters obtained from X-ray crystallography [REF DOI: 10.1055/a-2193-5436; Art ID: SS-2023-09-0389-OP]. The complex acquires a distorted octahedral geometry. The six donor sites include the 4 nitrogen atoms and 2 oxygen atoms of the ligands.

### 3.2. Frontier Molecular Orbital (FMO) analysis

The frontier molecular orbital analysis was performed to determine the global reactivity descriptors. The energy gap between frontier molecular orbitals (HOMO and LUMO) of a molecule is an important parameter to predict the stability and reactivity of the system. Various quantum chemical descriptors such as ionization potential (I) and electron affinity (A), global hardness ( $\eta$ ), global softness (S), electronegativity ( $\chi$ ), chemical potential ( $\mu$ ) and electrophilicity index ( $\omega$ ) of the molecule is computed and summarized in **Table 2**. The computed surface plots of HOMO and LUMO is displayed in **Figure 2**. The low band gap (4.250 eV) predicts the molecule to be kinetically stable and chemically reactive. The low band gap indicates facile charge

Mridula Guin, Kodipura P. Sukrutha, Kamakshi Sharma, Paratpar Sarkar, Ravani A. Roopa, Maralinganadoddi P. Sadashiva, Kuppalli R. Kiran

transfer process in the molecule. Again, the hardness value (2.125 eV) is quite low, signifying

the high reactivity of the molecule to alter the electron density.

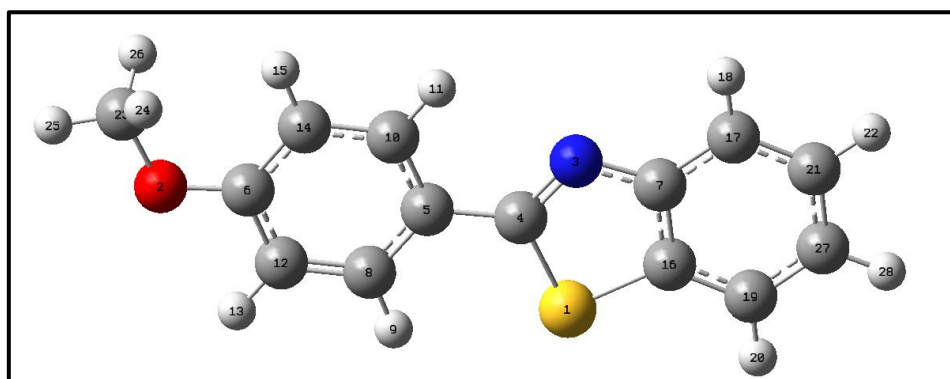


Figure 1. DFT optimized structure of the molecule.

**Table 1.** Selected bond lengths and bond angles of the DFT optimized geometry

Selected bonds	Bond lengths (Å)	Selected bond angles	Bond angles (°)
C23-O2	1.423	H25-C23-H24	109.38
O2-C6	1.360	H25-C23-O2	105.76
C6-C14	1.399	H24-C23-O2	111.31
C14-C10	1.391	C23-O2-C6	118.80
C10-C5	1.401	O2-C6-C12	115.85
C5-C8	1.405	O2-C6-C14	124.62
C8-C12	1.381	C14-C6-C12	119.53
C12-C6	1.401	C6-C14-C10	119.78
C5-C4	1.465	C14-C10-C5	121.30
C4-N3	1.296	C10-C5-C8	118.12
N3-C7	1.380	C5-C8-C12	121.11
C7-C16	1.414	C8-C12-C6	120.15
C16-S1	1.749	C5-C4-N3	124.25
C4-S1	1.789	C5-C4-S1	121.18
C7-C17	1.401	N3-C4-S1	114.56
C17-C21	1.388	C4-N3-C7	112.18
C21-C27	1.404	N3-C7-C16	113.33
C27-C19	1.391	N3-C7-C17	125.27
C19-C16	1.394	C7-C17-C21	119.08
C16-C7	1.414	C17-C21-C27	120.91
H25-C23	1.088	C21-C27-C19	120.94
H24-C23	1.095	C27-C19-C16	118.11
C14-H15	1.082	C19-C16-C7	121.55
C10-H11	1.083	C16-S1-C4	88.771
C12-H13	1.083	C6-C14-H15	121.04
C17-H18	1.083	C6-C12-H13	118.68
C21-H22	1.084	H15-C14-C10	119.18
C27-H28	1.084	H11-C10-C14	120.02
H20-C19	1.083	H11-C10-C5	118.67
		C5-C8-H9	120.21
		H9-C8-C12	118.67
		C8-C12-H13	112.16
		H13-C12-C6	118.68
		C7-C17-H18	119.29
		C21-C17-H18	121.62
		H22-C21-C27	119.43

Mridula Guin, Kodipura P. Sukrutha, Kamakshi Sharma, Paratpar Sarkar, Ravani A. Roopa, Maralinganadoddi P. Sadashiva, Kuppalli R. Kiran

		H28-C27-C19	119.37
		H20-C19-C16	121.19

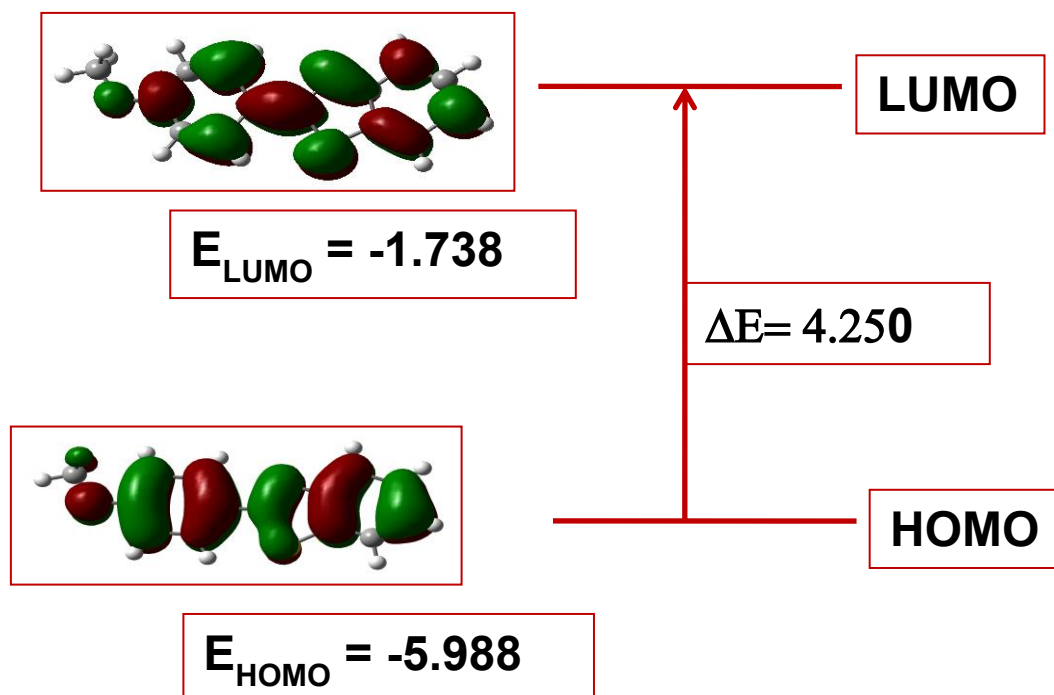


Figure 2. 3D surface plots of HOMO and LUMO of the molecule

Table 2. FMO energy parameters and global reactivity descriptors of the molecule.

Parameters	Values
HOMO (eV)	-5.988
LUMO (eV)	-1.738
$\Delta E = (\text{LUMO}-\text{HOMO})$ (eV)	4.250
$I = -E(\text{HOMO})(\text{eV})$	5.988
$A = -E(\text{LUMO})$ (eV)	1.738
$\chi = (I + A)/2$ (eV)	3.863
$\mu = -\chi$ (eV)	-3.863
$\eta = (I - A)/2$ (eV)	2.125
$S = 1/\eta$ (eV)	0.471
$\omega = \mu^2/2 \eta$ (eV)	3.511

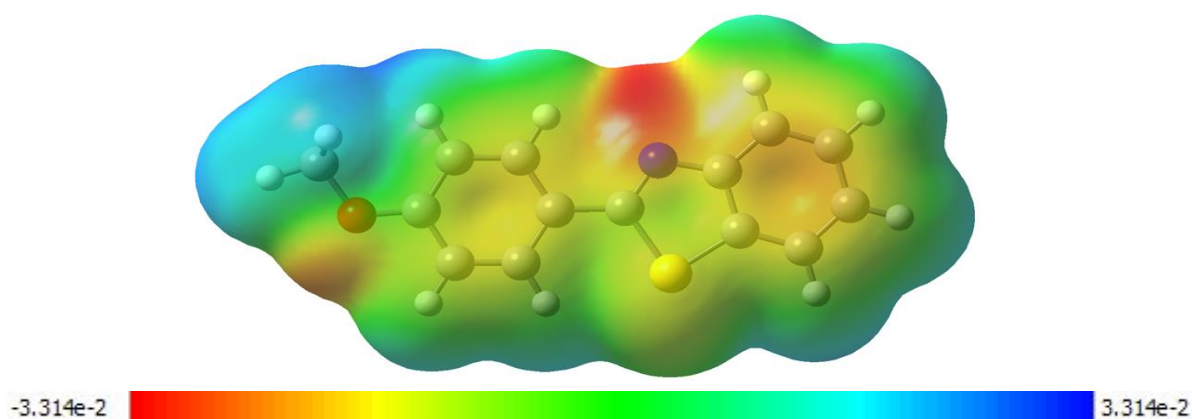


Figure 3. Molecular electrostatic potential map of the molecule

Mridula Guin, Kodipura P. Sukrutha, Kamakshi Sharma, Paratpar Sarkar, Ravani A. Roopa, Maralinganadoddi P. Sadashiva, Kuppalli R. Kiran

### 3.3. Molecular Electrostatic Potential (MEP)

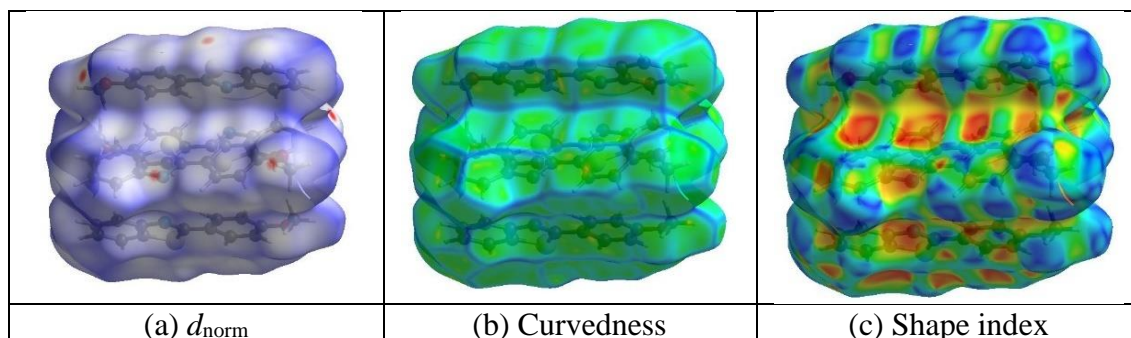
The electrostatic potential of a molecular entity is a valuable tool to predict electrophilic and nucleophilic sites within the molecule. The propensity of formation of various types of intermolecular interactions, for example: hydrogen bonding, drug-receptor interaction, enzyme-substrate interactions etc is majorly based on the electrostatic potential of the molecule [31]. The MEP of the metal complex is calculated using electron density of the optimized structure and displayed in **Figure 3**. The 3D map highlights the electron density in terms of different colour in increasing order blue<green<yellow<orange<red. The figure indicates the presence of high electron density or negative charge around the nitrogen and oxygen atom of the molecules (red colored surface) as strong nucleophilic region. While the sulphur atom and phenyl rings are yellowish colour indicating moderately nucleophilic reactivity on those sites. the methyl group displays blue surface indicating electron deficiency. Thus, the electrophilic reactivity of the complex will be centered around the methoxy group.

### 3.4. Hirshfeld surface analysis

The Hirshfeld surfaces of the compound mapped in terms of  $d_{\text{norm}}$ , curvedness and shape index are shown in **Figure 4**. The  $d_{\text{norm}}$  surface represents the normalized contact distance. Several red spots in the  $d_{\text{norm}}$  surface indicates the atoms present in close proximity to the inner and outer side of Hirshfeld surface arising due to the N···H, O···H, S···H, and C···H intermolecular interactions. The low intensity of the red colour spots indicates the weak nature of these intermolecular contacts in the studied molecule. The white and blue surfaces indicate

atoms with medium proximity and large distance respectively from the Hirshfeld surface. The shape index and curvedness determine the shape and surface area of the molecule. The shape index is a key parameter in understanding the presence of  $\pi$ - $\pi$  stacking interactions in the packing modes of the crystal [32]. The shape index surface shows adjacent red and blue triangles indicating the presence of adjacent concave and convex region. This implies that the molecular crystal is stabilized with weak  $\pi$ - $\pi$  stacking interactions. Further the curvedness map supports the findings of shape index. The presence of flat surface patches in the curvedness map clearly tells that the crystal is packed with  $\pi$ - $\pi$  stacking interactions.

The two-dimensional fingerprint plots (**Figure 5**) of the major contacts are determined to quantify the intermolecular interactions. The molecular crystal is mostly packed with H···H and C···H contacts as major interactions contributing about 46.7% and 29.4% respectively to the overall crystal packing. The absence of characteristic wing feature with bow-tie pattern of C···H contacts indicate the absence of C-H··· $\pi$  interaction in the crystal [33-36]. Additionally, O···H and N···H contacts are also observed stabilizing the crystal through hydrogen bonding interaction. Both O···H and N···H contacts in the FP plots are noticed with their signature symmetrical sharp spikes. The sharpness of N···H contacts are more than that of O···H advocating the stabilization of the molecular crystal with strong N···H hydrogen bonding interactions compared to O···H contacts [37]. Other interactions with minor contribution in the crystal packing are C···S and S···S interactions, contributing 2.1% and 1.3% respectively to the packing of the crystal.



Mridula Guin, Kodipura P. Sukrutha, Kamakshi Sharma, Paratpar Sarkar, Ravani A. Roopa, Maralinganadoddi P. Sadashiva, Kuppalli R. Kiran

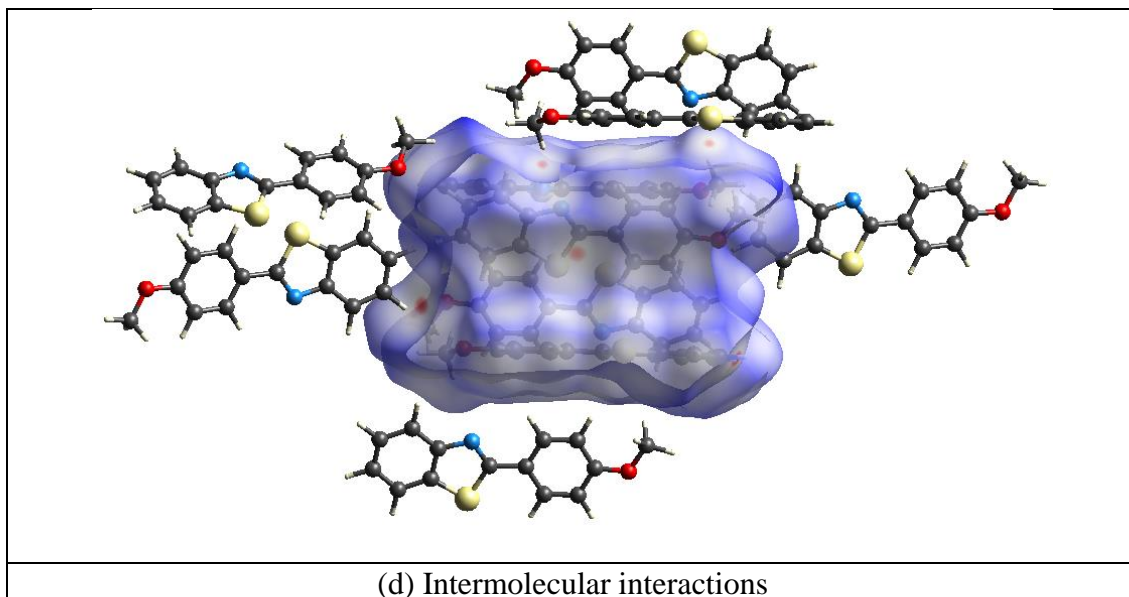
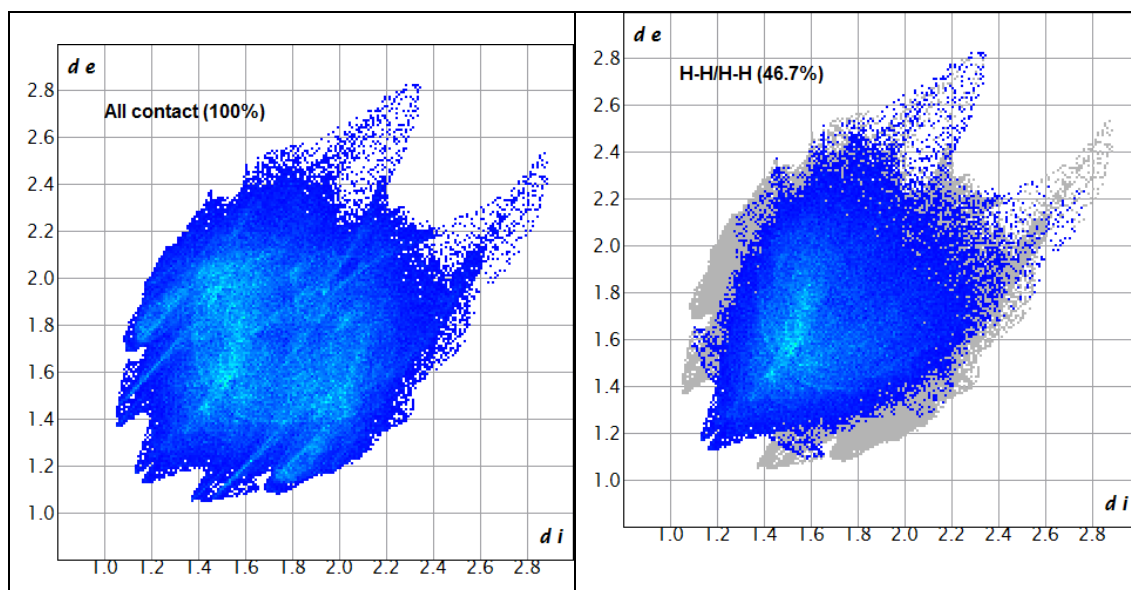


**Figure 4.** Hirshfeld surfaces mapped over (a)  $d_{\text{norm}}$ , (b) curvedness (c) shape index and (d) intermolecular interactions.



Mridula Guin, Kodipura P. Sukrutha, Kamakshi Sharma, Paratpar Sarkar, Ravani A. Roopa, Maralinganadoddi P. Sadashiva, Kuppalli R. Kiran

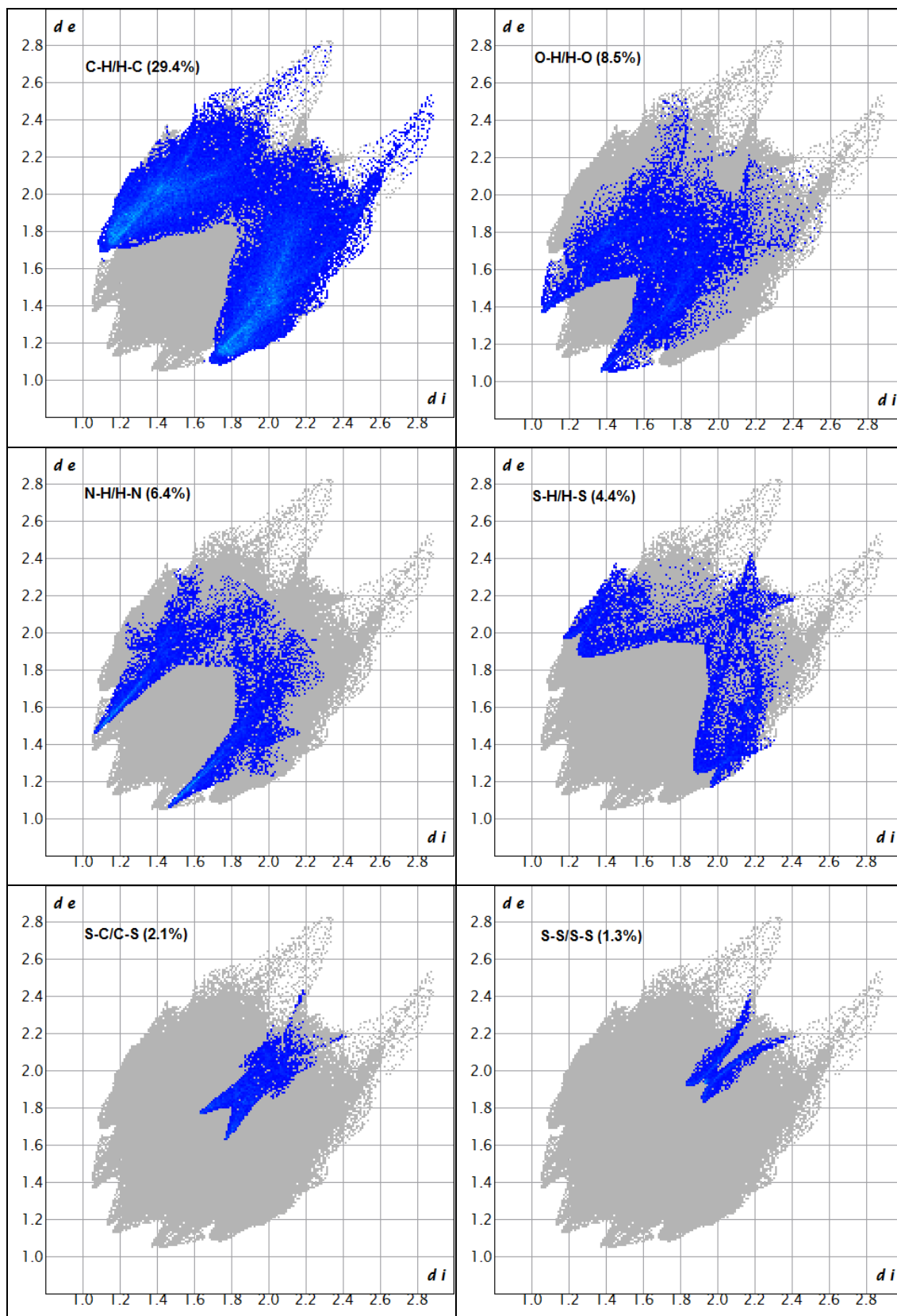


**Figure 5.** Two-dimensional fingerprint plot of the molecule showing the contributions of individual interactions.

Mridula Guin, Kodipura P. Sukrutha, Kamakshi Sharma, Paratpar Sarkar, Ravani A. Roopa, Maralinganadoddi P. Sadashiva, Kuppalli R. Kiran

### 3.5. Molecular docking

The ligand 2-(4-methoxyphenyl)benzo[d]thiazole is docked strongly with Metastasis factor (S100A4)(PDB ID: 2Qp 1) with an overall binding energy of -79.8 kcal/mol. The amount of high binding energy correlates a strong binding affinity between the ligand and the receptor. This is a member of small calcium-binding protein family and is involved in the cell proliferation and cancer progression. The amino acid of the receptor involved in interaction with the ligand is an acidic amino acid Glutamic acid. Molecular docking of 2-(4-methoxyphenyl)benzo[d]thiazole against second cancer receptor, myotonic dystrophy-related Cdc42-binding kinases(MRCK beta in complex with fusadil) with PDB Id: 3ktu releases a slightly lower binding energy of -67.8 kcal/mol. The amino acids involved in the interaction is phenyl alanine and it forms a hydrogen bond with the receptor. The same ligand when docked with the third receptor. myotonic dystrophy-related Cdc42-binding kinases (MRCK beta in complex with fusadil) releases an

equivalent to -71.4kcal/mol. Here only amino acid glutamine is involved in hydrogen interaction with the receptor. However the same ligand docked very strongly with the fourth cancer regulating receptor, adhesion GPCR ADGRL3 with a binding energy of -78kcal/mol. One non polar amino leucine and another polar amino acid serine is involved in the interaction with the protein. G Protein Coupled Receptors (GPCRs) perceive many extracellular signals and transduce them to heterotrimeric G proteins, which further transduce these signals intracellularly to appropriate downstream effectors and thereby play an important role in various signalling pathways and also an important role in the initiation of cancer. Our docking study shows that the ligand, 2-(4-methoxyphenyl)benzo[d]thiazole is stable enough to bind strongly with the two cancer receptor (1. Metastasis factor (S100A4) 2. adhesion GPCR ADGRL3) and can modulate the signalling of the cancer protein that can alter the behaviour and pattern of cancer initiation in the body.

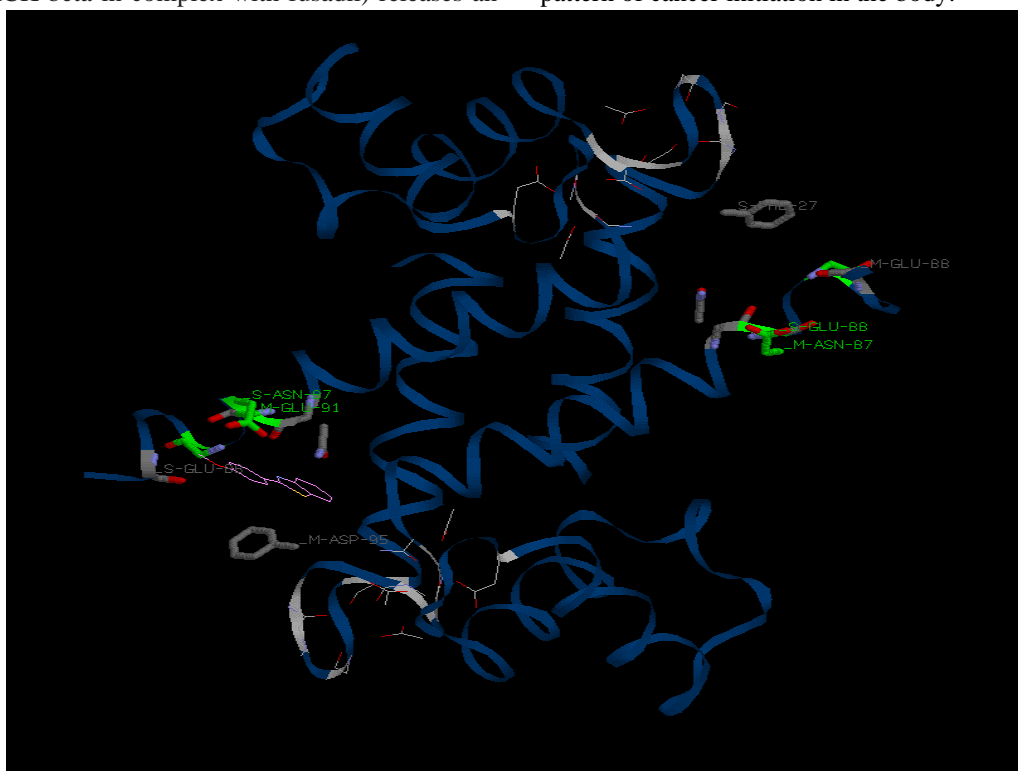


**Figure 6.** Molecular docking of 2-(4-methoxyphenyl)benzo[d]thiazole against calcium bound metastatic factor (PDB ID: 2q91).

**Table 3.** Amino acids involved in the interaction of 2-(4-methoxyphenyl)benzo[d]thiazole with calcium bound metastatic factor

Mridula Guin, Kodipura P. Sukrutha, Kamakshi Sharma, Paratpar Sarkar, Ravani A. Roopa, Maralinganadoddi P. Sadashiva, Kuppalli R. Kiran

SN.	Compound	Amino acid involved in covalent interaction			
		Hydrogen bond (kcal/mol)		van deer Waal energy (kcal/mol)	
1.		<b>Amino acid</b>	<b>Energy</b>	<b>Amino acid</b>	<b>Energy</b>
	Overall energy = -79.8 (kcal/mol)	H-S-GLU-88	-2.5	V-M-ASN-87	-4.9
		H-M-GLU-91	-3.4	V-S-ASN-87	-6.1
				V-M-GLU-88	-5.7
				V-S-GLU-88	-5.4
				V-M-ASP-95	-4.7
				V-S-PHE-27	-10.4

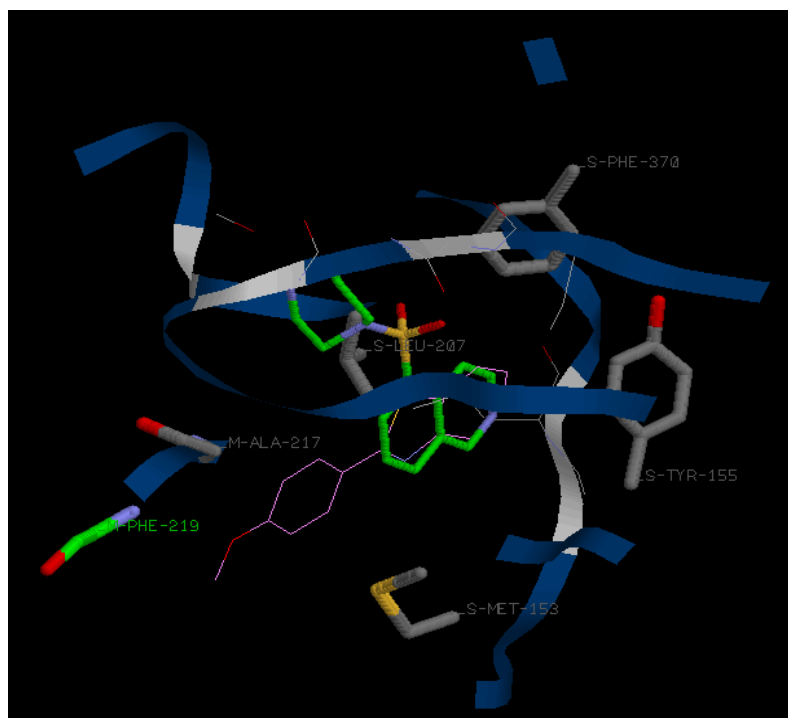


**Figure 7.** Molecular docking of 2-(4-methoxyphenyl)benzo[d]thiazole against myotonic dystrophy-related Cdc42-binding kinases (MRCK beta in complex with fusadil) with PDB Id: 3ktu.

**Table 4.** Amino acids involved in the interaction of 2-(4-methoxyphenyl)benzo[d]thiazole with myotonic dystrophy-related Cdc42-binding kinases.

SN.	Compound	Amino acid involved in covalent interaction			
		Hydrogen bond (kcal/mol)		van deer Waal energy (kcal/mol)	
1.		<b>Amino acid</b>	<b>Energy</b>	<b>Amino acid</b>	<b>Energy</b>
	Overall energy = -67.5 (kcal/mol)	H-M-PHE-219	-3.5	V-S-MET-153	-4.3
				V-S-TYR-155	-4.2
				V-S-LEU-207	-4.5
				V-M-ALA-217	-4.8
				V-S-PHE-370	-4.1

Mridula Guin, Kodipura P. Sukrutha, Kamakshi Sharma, Paratpar Sarkar, Ravani A. Roopa, Maralinganadoddi P. Sadashiva, Kuppalli R. Kiran

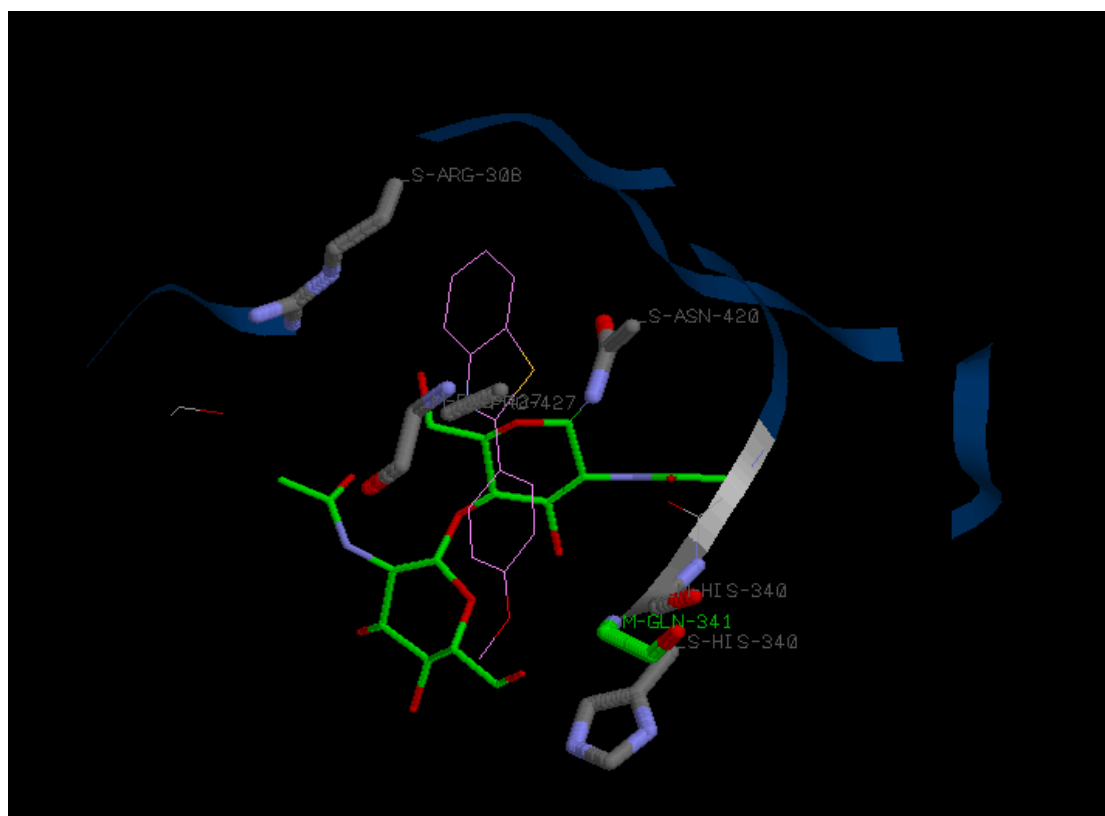


**Figure 8.** Molecular docking of 2-(4-methoxyphenyl)benzo[d]thiazole against an engineered Axl 'decoy receptor with a PDB ID: 4raO.

**Table 5.** Amino acids involved in the interaction of 2-(4-methoxyphenyl)benzo[d]thiazole with myotonic dystrophy-related Cdc42-binding kinases.

SN.	Compound	Amino acid involved in covalent interaction			
		Hydrogen bond (kcal/mol)		van deer Waal energy (kcal/mol)	
1.	Overall energy = -71.4 (kcal/mol)	Amino acid	Energy	Amino acid	Energy
		H-M-GLN-341	-3.5	V-S-ARG-308	-8.8
				V-M-HIS-340	-4.5
				V-S-HIS-340	-4.2
				V-S-ASN-420	-9.5
				V-M-PRO-427	-4.7
				V-S-PRO-427	-4.6

Mridula Guin, Kodipura P. Sukrutha, Kamakshi Sharma, Paratpar Sarkar, Ravani A. Roopa, Maralinganadoddi P. Sadashiva, Kuppalli R. Kiran

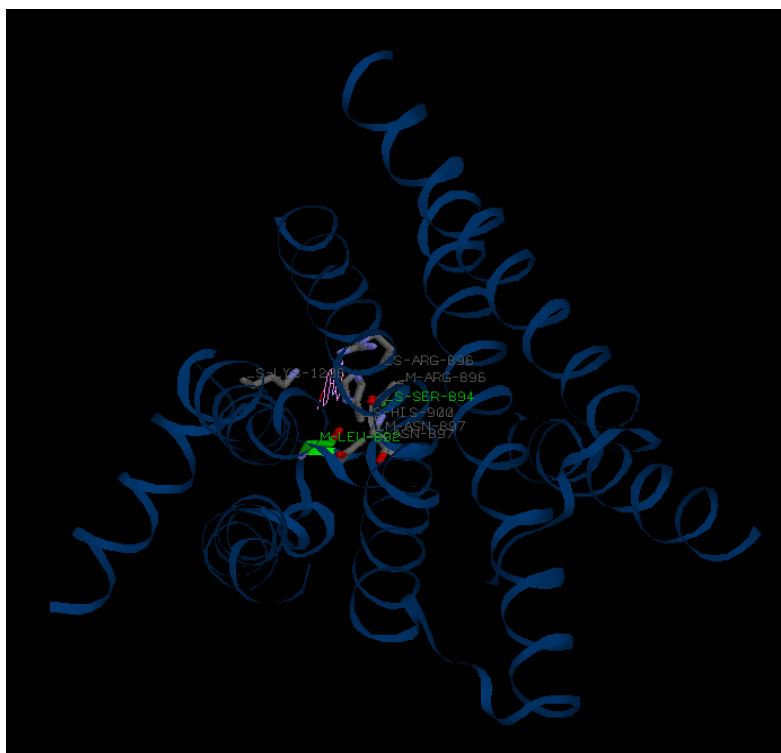


**Figure 9.** Molecular docking of 2-(4-methoxyphenyl)benzo[d]thiazole against adhesion GPCR ADGRL3 with a PDB ID: 8jmt

**Table 6.** Amino acids involved in the interaction of 2-(4-methoxyphenyl)benzo[d]thiazole with adhesion GPCR ADGRL3

SN.	Compound	Amino acid involved in covalent interaction			
		Hydrogen bond (kcal/mol)		van deer Waal energy (kcal/mol)	
1.		<b>Amino acid</b>	<b>Energy</b>	<b>Amino acid</b>	<b>Energy</b>
	Overall energy = -78 (kcal/mol)	H-M-LEU-892	-3.5	V-M-LEU-892	-6.4
		H-S-SER-894	-3.5	V-M-ARG-896	-7.1
				V-S-ARG-896	-8
				V-M-ASN-897	-5.1
				V-S-HIS-900	-4.2
				V-S-LYS-1206	-7.2

### 3.6. Drug likeness and ADMET prediction

#### Drug likeness and ADMET study

For a drug candidate, biological activity, ADMET properties and pharmacokinetic profile is the foremost parameter to know for its application in medicinal field. The absorption of a drug inside body and there its efficacy is predicted by the thumb rule known as Lipinski's rule of five. The percentage of plasma concentration is indicated by the bioavailability score. The passive transport system of cell membranes is directly related to the hydrogen bonding and can be understood from the value of topological polar surface area (TPSA). The

drug likeness, bioactivity score and ADMETox properties of the compounds are predicted using molinspiration [38] and ADMETSAR [39] online servers. A number of druglike properties such as hydrophobicity (logP), aqueous solubility (logS) kinase inhibition, protease inhibition, nuclease receptor ligand, GPCRL and ion channel modulation are predicted. Further, pharmacokinetic characteristics like absorption, distribution, metabolism, excretion and toxicity profile of ligand and complexes are recorded in the form of Caco-2 cell permeability, blood-brain barrier (BBB) permeability, human intestinal absorption (HIA),

Mridula Guin, Kodipura P. Sukrutha, Kamakshi Sharma, Paratpar Sarkar, Ravani A. Roopa, Maralinganadoddi P. Sadashiva, Kuppalli R. Kiran

and toxicity parameters, such as carcinogenicity, mutagenicity, LD50 dose, and so forth. All these *in-silico* predicted data are compared with the two reference drugs riluzole and gefitinib.

Drug likeness and bioactivity scores of the compound is shown in **Table 7**. It can be seen from the drug likeness properties that the molecule obeys Lipinski's rule without any violation. The TPSA, mlogP values of the ligand is within the allowable range of the candidate drug to penetrate the bio membrane, and show good bioavailability degree. TPSA of the molecule lies well below the limit of 140Å<sup>2</sup>. The bioactivity score of the compound is also predicted by Molinspiration cheminformatics software. A positive bioactivity score predicts the compound to show significant biological activity. While a compound having a score between -0.5 to 0.0 is said to be moderately active and score less than zero suggest an inactive compound. The score in **Table 7**, suggest that the molecule is moderately bioactive.

The results of the ADMET study shown in **Table 8** reveal that the compound has good absorption

and distribution characteristics. The human intestinal absorption (HIA) of this molecule is better than the reference drugs predicting the molecule as potent drug candidate. The Caco-2 permeability value 0.5758, indicates good absorption. The BBB value 0.9575 as per in the range of approved reference drugs. The predicted value of permeability of HIA, BBB and Caco-2 is in high, which indicates their good pharmacokinetics. The compounds are predicted to be non-carcinogenic but AMES mutagenic. The median lethal dose (LD50) value calculated in the rat model helps determine the lethality of the compound. It was found that the LD<sub>50</sub> value of the compound is 1.708 mol/kg which is lower than the two reference drugs that are compared in this study suggesting it as better therapeutic agent. The drug likeness and ADMET properties of the compounds are as per with two approved drugs riluzole and gefitinib.

**Table 7.** Summarized drug likeness and bioactivity profile of the molecule (Molinspiration)

	Parameters	Compound	Riluzole	Gefitinib
<b>Druglikeness</b>	<b>miLogP</b>	4.35	2.92	4.19
	<b>TPSA</b>	22.13	48.15	68.75
	<b>Nviolations</b>	0	0	0
	<b>Natoms</b>	17	15	31
	<b>MW</b>	241.31	234.20	446.91
	<b>nON</b>	2	3	7
	<b>nOHNH</b>	0	2	1
	<b>Nrotb</b>	2	2	8
<b>Bioactivity scores</b>	<b>Volume</b>	211.54	166.16	385.07
	<b>GPCRL</b>	-0.59	-0.52	0.12
	<b>ICM</b>	0.058	-0.04	-0.04
	<b>KI</b>	-0.16	-0.31	0.66
	<b>NRL</b>	-0.51	-0.80	-0.21
	<b>PI</b>	-0.67	-0.60	-0.30
	<b>EI</b>	-0.23	-0.21	0.03

**Table 8: The ADMET properties and toxicity analysis of all four molecules (ADMETSAR)**

	BBB	HIA	Caco-2 Permeability	Renal Organic cation transporter	AMES Toxicity	Carcinogenicity	Rat acute Toxicity LD <sub>50</sub> mol/kg
Compound	0.9575	1.0000	0.5758	Non-Inhibitor	Toxic	Non-carcinogens	1.7080
Riluzole	0.9799	0.9950	0.5377	Non-Inhibitor	Toxic	Non-carcinogens	3.6843
Gefitinib	0.9759	0.9961	0.5934	Inhibitor	Non toxic	Non-carcinogens	2.5141

Mridula Guin, Kodipura P. Sukrutha, Kamakshi Sharma, Paratpar Sarkar, Ravani A. Roopa, Maralinganadoddi P. Sadashiva, Kuppalli R. Kiran

#### 4. Conclusions

This study involves the theoretical calculation of 2-(4-methoxyphenyl)benzo[d]thiazole based on DFT approach. Theoretical predicted structure is found to be in good correlation with the experimentally attained structure obtained from XRD. The FMO analysis suggest the molecule to be kinetically stable and chemically reactive. The band gap was found to be 4.5 eV supporting facile electron transfer in the molecule. The MEP map indicates the presence of high electron density or strong nucleophilic region of around the nitrogen and oxygen atom of the molecules. The area near the sulphur atom and phenyl rings will show moderate nucleophilic reactivity while the electrophilic reactivity of the complex will be centred around the methoxy group. The Hirshfeld surface analysis shows the presence of N...H, O...H, S...H, and C...H inter-molecular interactions accounting for the stability of the molecular crystal. The nature of both shape index and curvedness surface implies that the molecular crystal to be stabilized with weak  $\pi$ - $\pi$  stacking interactions. The two-dimensional fingerprint plots show H...H and C...H interactions as major contacts contributing about 46.7% and 29.4% respectively to the overall crystal packing. In addition, O...H and N...H hydrogen bonding interaction also contribute significantly in crystal packing. The drug likeness and ADMET properties of the compound support good bioactivity and non-toxicity of the compound. Molecular docking studies prove the molecule to bind strongly with the two-cancer receptor to modulate the signalling of the cancer protein. This result supports the potential of the compound as an effective anticancer agent and pave the way for further investigations and potential applications in the development of new anticancer agent.

#### ACKNOWLEDGEMENT

**Conflict of interest:** The authors declare that they have no conflict of interest.

#### Author Contribution

Mridula Guin and Kodipura P. Sukrutha both the authors have equal contributions.

#### References

- [1] Keri R S, Patil M R, Patil S A, & Budagumpi S, A comprehensive review in current developments of benzothiazole-based molecules in medicinal chemistry.
- [2] Eur. J. Med. Chem 8 (2015) 207-251.
- [3] Seth S, A comprehensive review on recent advances in synthesis & pharmacotherapeutic potential of benzothiazoles. *Antiinflamm Antiallergy Agents Med Chem* 1 (2015) 498-112.
- [4] Yadav K P, Rahman M A, Nishad S, Maurya S K, Anas M, & Mujahid M, Synthesis and biological activities of benzothiazole derivatives: A review. *Intelligent Pharm* 1 (2023) 122-132.
- [5] Amir M, Hassan Z, Functional roles of benzothiazole motif in antiepileptic drug research. *Mini Rev Med Chem* 13 (2013) 2060-2075.
- [6] Weekes, A. A., & Westwell, A. D. (2009). 2-Arylbenzothiazole as a privileged scaffold in drug discovery. *Curr. Med. Chem*, 16(19), 2430-2440.
- [7] Sunny S, John S E, Shankaraiah N, Exploration of C-H Activation Strategies in Construction of Functionalized 2-Aryl Benzoazoles: A Decisive Review. *Asian J Org Chem* 10 (2021) 1986-2009.
- [8] Azzam R A, Osman R R, Elgemeie G H, Efficient synthesis and docking studies of novel benzothiazole-based pyrimidine sulfonamide scaffolds as new antiviral agents and Hsp90 $\alpha$  inhibitors. *ACS Omega* 5 (2020) 1640-1655.
- [9] Hu R, Li X, Tong Y, Miao D, Pan Q, Jiang Z, Han, S, Catalyst-Free synthesis of 2-Arylbenzothiazoles in an air/DMSO Oxidant System. *Synlett* 27 (2016) 138.
- [10] Gill R K, Rawal R K, Bariwal J, Recent advances in the chemistry and biology of benzothiazoles. *Archiv der Pharmazie* 348 (2015) 55-178.
- [11] Gao X, Liu J, Zuo X, Feng X, Gao Y, Recent advances in synthesis of benzothiazole compounds related to green chemistry. *Molecules* 25 (2020) 1675.
- [12] García-Báez E. V, Padilla-Martínez I I, Tamay-Cach F, Cruz, A, Benzothiazoles from condensation of o-aminothiophenoles with

**Mridula Guin, Kodipura P. Sukrutha, Kamakshi Sharma, Paratpar Sarkar, Ravani A. Roopa, Maralinganadoddi P. Sadashiva, Kuppalli R. Kiran**

- carboxylic acids and their derivatives: A review. *Molecules* 26 (2021) 6518.
- [13] Hutchinson I, Stevens M F, Westwell A D, The regiospecific synthesis of 5-and 7-monosubstituted and 5, 6-disubstituted 2-arylbenzothiazoles. *Tetrahedron Lett* 41 (2000) 425-428.
- [14] Benedí C, Bravo F, Uriz P, Fernández E, Claver C, Castillón, S, Synthesis of 2-substituted-benzothiazoles by palladium-catalysed intramolecular cyclization of o-bromophenylthioureas and o-bromophenylthioamides. *Tetrahedron Lett* 44 (2003) 6073-6077.
- [15] Zhang X, Zeng W, Yang Y, Huang H, Liang Y, Copper-catalysed double C–S bonds formation via different paths: synthesis of benzothiazoles from N-benzyl-2-iodoaniline and potassium sulfide. *Org Lett* 16 (2014) 876-879.
- [16] Wang B, Zhang Q, Guo Z, Ablajan K, Iodine- and TBHP-promoted acylation of benzothiazoles under metal-free conditions. *Synthesis* 52 (2020) 3058-3064.
- [17] Huang Y, Zhou P, Wu W, Jiang H, Selective construction of 2-substituted benzothiazoles from o-iodoaniline derivatives S8 and N-tosyl hydrazones. *J Org Chem* 83 (2018) 2460-2466.
- [18] Zhu X, Zhang F, Kuang D, Deng G, Yang Y, Yu J, Liang Y, K<sub>2</sub>S as sulfur source and DMSO as carbon source for the synthesis of 2-unsubstituted benzothiazoles. *Org Lett* 22 (2020) 3789-3793.
- [19] Yadong S, Huanfeng J, Wanqing W, Wei Z, Xia W, Copper-Catalysed Synthesis of Substituted Benzothiazoles via Condensation of 2-Aminobenzenethiols with Nitriles. *Org Lett* 15 (2013) 1598–1601.
- [20] Xu W, Zeng M T, Liu M, Liu S S, Li Y S, Dong Z, Palladium-catalysed synthesis of 2-aminobenzothiazoles through tandem reaction. *Synthesis* 49 (2017) 3084-3090.
- [21] Lewars E, Computational chemistry. In *Introduction to the Theory and Applications of Molecular and Quantum Mechanics* Springer Berlin/Heidelberg Germany (2003) 318.
- [22] Ramachandran K, Deepa G, Namboori, K, Computational chemistry and molecular modelling: Principles and applications. Springer Science & Business Media Berlin/Heidelberg Germany (2008).
- [23] Malashkevich V N, Varney K M, Garrett S C, Wilder P T, Knight D, Charpentier T H, Ramagopal U A, Almo S C, Weber D J, Bresnick A R, Structure of Ca<sup>2+</sup> bound S100A4 and its interaction with peptides derived from nonmuscle myosin-IIA. *Biochemistry* 47 (2008) 5111-5126.
- [24] Heikkila T, Wheatley E, Crighton D, Schroder E, Boakes A, Kaye S J, Mezna M, Pang L, Rushbrooke M, Turnbull A, Olson, M F, Co-crystal structures of inhibitors with MRCK $\beta$ , a key regulator of tumour cell invasion. *PLoS One* 6 (2011) 24825.
- [25] Kariolis M S, Miao Y R, Jones D S, Kapur S, Mathews I I, Giaccia A J, Cochran J R, An engineered Axl'decoy receptor' effectively silences the Gas6-Axl signalling axis. *Nature Chem Biol* 10 (2014) 977-983.
- [26] Guo Q, He B, Zhong Y, Jiao H, Ren Y, Wang Q, Ge Q, Gao Y, Liu X, Du Y, Hu H, A method for structure determination of GPCRs in various states. *Nature Chem Biol* 20 (2024) 74-82.
- [27] Gaussian 16, Revision C.01, Frisch, M. J.; Trucks, G. W.; Schlegel, H. B.; Scuseria, G. E.; Robb, M. A.; Cheeseman, J. R.; Scalmani, G.; Barone, V.; Petersson, G. A.; Nakatsuji, H.; Li, X.; Caricato, M.; Marenich, A. V.; Bloino, J.; Janesko, B. G.; Gomperts, R.; Mennucci, B.; Hratchian, H. P.; Ortiz, J. V.; Izmaylov, A. F.; Sonnenberg, J. L.; Williams-Young, D.; Ding, F.; Lipparini, F.; Egidi, F.; Goings, J.; Peng, B.; Petrone, A.; Henderson, T.; Ranasinghe, D.; Zakrzewski, V. G.; Gao, J.; Rega, N.; Zheng, G.; Liang, W.; Hada, M.; Ehara, M.; Toyota, K.; Fukuda, R.; Hasegawa, J.; Ishida, M.; Nakajima, T.; Honda, Y.; Kitao, O.; Nakai, H.; Vreven, T.; Throssell, K.; Montgomery, J. A., Jr.; Peralta, J. E.; Ogliaro, F.; Bearpark, M. J.; Heyd, J. J.; Brothers, E. N.; Kudin, K. N.;

Mridula Guin, Kodipura P. Sukrutha, Kamakshi Sharma, Paratpar Sarkar, Ravani A. Roopa, Maralinganadoddi P. Sadashiva, Kuppalli R. Kiran

- Staroverov, V. N.; Keith, T. A.; Kobayashi, R.; Normand, J.; Raghavachari, K.; Rendell, A. P.; Burant, J. C.; Iyengar, S. S.; Tomasi, J.; Cossi, M.; Millam, J. M.; Klene, M.; Adamo, C.; Cammi, R.; Ochterski, J. W.; Martin, R. L.; Morokuma, K.; Farkas, O.; Foresman, J. B.; Fox, D. J. Gaussian, Inc., Wallingford CT, 2016.
- [28] Wiberg, K.B., Basis set effects on calculated geometries: 6-311++G\*\* vs. aug-cc-pVDZ. *J Comp Chem* 25 (2004) 1342. <https://doi.org/10.1002/jcc.20058>.
- [29] Mubarik A, Mahmood S, Rasool N, Hashmi M A, Ammar M, Mutahir S, Ali K G, Bilal M, Akhtar M N, Ashraf G, Computational study of benzothiazole derivatives for conformational, thermodynamic and spectroscopic features and their potential to act as antibacterials. *Crys 12 A* (2022) 912.
- [30] Turner M J, McKinnon J J, Wolff S K, Grimwood D J, Spackman P R, Jayatilaka D, Spackman M A, Crystal Explorer17. The University of Western Australia (2017).
- [31] Hsu K C, Chen Y F, Lin S R, Yang J M, I GEMDOCK: a graphical environment of enhancing GEMDOCK using pharmacological interactions and post-screening analysis. *BMC Bioinform* 12 (2011) 1-11.
- [32] Lakshminarayanan S, Jeyasingh V, Murugesan K, Selvapalam N, Dass G, Molecular electrostatic potential (MEP) surface analysis of chemo sensors: An extra supporting hand for strength, selectivity & non-traditional interactions. *J Photochem Photobiol* 6 (2021) 100022.
- [33] Spackman M A, Dylan J, Hirshfeld surface analysis. *Cryst Eng Comm.*11 (2009) 19-32.
- [34] Mridula G, Shibashis H, Sudipta C, Saugata K, Synthesis, X-ray crystal structure of Cu(II) 1D coordination Polymer: In View of Hirshfeld surface, FMO, Molecular electrostatic potential (MEP) and Natural Bond orbital (NBO) analyses. *J Mol Struc* 1270 (2022) 133949.
- [35] De A, Kathait M A, Jain P, Guin M, DFT Investigation, Hirshfield Analysis and Molecular Docking of Cu (II) Complex of O-Vanillin Based Ligand. *Chem Select* 7(2022) e202202884.
- [36] Sadeka J M, Mridula G, Suman K, Sujit B K, Synthesis, Structures and Hirshfeld surface analysis of Ni (II) and Co (III) complexes with N=2O donor Schiff base ligand. *J Ind Chem Soc* 98 (2021) 100080.
- [37] Ashfaq M, Munawar K S, Tahir M N, Dege N, Yaman M, Muhammad S, Alarfaji S S, Kargar H, Arshad M U, Synthesis, crystal structure, Hirshfeld surface analysis, and computational study of a novel organic salt obtained from benzylamine and an acidic component. *ACS Omega* 6 (2021) 22357-22366.
- [38] Mridula Guin, Kamal Rautela, Roopa R.A, Shantharam, C.S. Begam Elavarasi S, Hydrogen bonded complexes of rhodanine with H<sub>2</sub>X/CH<sub>3</sub>XH (X = O, S, Se). *Comput. Theor. Chem.* 1196 (2021) 113134.
- [39] Molinspiration C. Calculation of molecular properties and bioactivity score. <http://www.molinspiration.com/cgi-bin/properties> 2011.
- [40] Cheng F, Li W, Zhou Y, Shen J, Wu Z, Liu G, Lee P W, Tang Y, A comprehensive source and free tool for evaluating chemical ADMET properties. *J Chem Inf Model* 52 (2012) 3099.